THEORETICAL & APPLIED MECHANICS LETTERS **4**, 021008 (2014)

Microstructural and mechanical properties of thermal barrier coating at 1400°C treatment

Jianguo Zhu,[1, a)] Kang Ma[2, b)]
[1)] *Faculty of Civil Engineering and Mechanics, Jiangsu University, Zhenjiang 212013, China*
[2)] *AML, Department of Engineering Mechanics, Tsinghua University, Beijing 100084, China*

(Received 10 November 2013; revised 9 December 2013; accepted 3 January 2014)

Abstract The mechanical properties of plasma-sprayed thermal barrier coating (TBC) play a vital role in governing their lifetime and performance. This work investigated the microstructural and mechanical properties of TBC with high temperature treatment at 1 400°C by scanning electron microscopy and indentation. We calculated elastic modulus and hardness through the application of Weibull statistics analysis. The results indicate that the microstructure of ceramic coating will change continuously at high temperature, and accordingly the porosity decreases due to the grain growths and crack closes. In addition, the elastic modulus and hardness nonlinearly go up with the heat treatment time and go down with increasing porosity. This demonstrates that the microstructural evolution and porosity of TBC are caused by high temperature treatment, and as a result its mechanical properties are influenced.

 [doi:10.1063/2.1402108]

Keywords thermal spray coating (TBC), mechanical property, mircrostructure, indentation

Thermal barrier coating systems (TBCs) are widely used in industrial gas-turbine engines to provide lubrication and thermal insulation for combustor engine components from the hot gas stream. However, the premature spallation-failure of TBC will expose the metallic substrate to the dangerous hot gases, which has impaired the use and shortened the lifetime of TBCs. The progressively changing mechanical properties of TBC lead to the misfit stress among the multilayer structures, which is one of the main factors responsible for the failures of TBCs.[1] Therefore, a better interpreting of the complex changes in the properties and structure is required for improvements in TBCs.

There are substantial researches on the mechanical properties of TBCs. Since 1990s, the mechanical behavior of TBCs at room temperature had been investigated using various test methods, including bending,[2] resonant frequency,[3] and indentation.[4] The mechanical properties of TBC exposed to high temperature were also studied. Qi et al.[5] investigated the elastic modulus of 1 050°C isothermal ceramic coatings using indentation technique. Guo and Kagawa[6] measured the ceramic coatings and thermally growth oxide after 1 150°C high temperature exposure to an oxidizing atmosphere. Choi et al.[7] measured the mechanical behavior for plasma-sprayed thermal barrier coatings. The specimens were first heated at 800°C and 1 316°C for a period of time, and then the mechanical properties of specimens were tested at room temperature.

[a)] Corresponding author. Email: zjg0511@gmail.com.
[b)] Email: jcmkang@163.com.

In this work, TBC specimens were fabricated with *w*(yttria) = 8% partially stabilized zirconia powder deposition on the Ni-based superalloy substrate. The free-standing ceramic coatings were obtained after the specimens were corroded in aqua regia for about an hour. The final specimen size is 60 mm × 10 mm × 1 mm (length × width × thickness). Then the specimens were put into a high temperature furnace for 1 400°C isothermal cycling treatment. The heating rate was 600°C per hour, while the cooling rate was about 200°C per hour, namely the specimens all had a heating and cooling experience in addition to the heat preservation time.

Figure 1 illustrates the scanning electron microscopy (SEM) diagrams of ceramic coating for different heat treatment time. Figure 1(a) shows the corrugated morphology of the as-received plasma-sprayed ceramic coating. The molten ceramic particles bond together during the coating building-up and the cracks are irregular with width less than 0.4 μm. The cracks will shrink or partially close due to the growth of small grains or recrystallization as a result of the sintering of coatings when exposed to the high temperature environment for a period of time. After heat treatment of 10 h, the surface becomes compact, fine, and close.

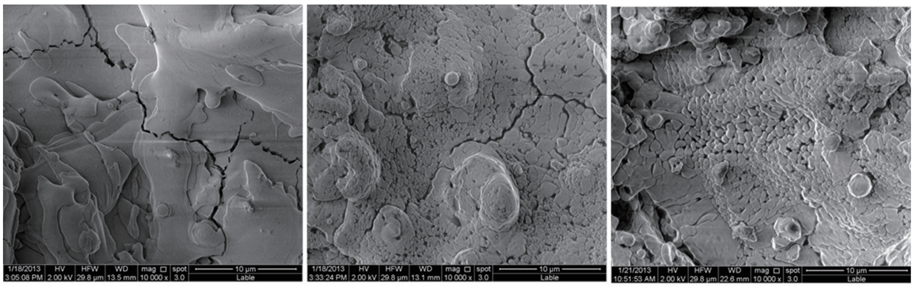

(a) As-received (b) 2 h (c) 10 h

Fig. 1. SEM diagrams of ceramic coating for different heat treatment times.

The porosities and densities were tested in accordance with the ASTM C20-00.[8] Figure 2 shows the curve of porosity versus heat treatment time. Each data point was obtained from the average of three specimens. The porosity of as-received coating is about 8.5%. The porosity decreases quickly with the heat treatment time in the beginning 5 h, and decreases slowly afterwards. The porosity with 20 h heat treatment time is about 5.8%. The results can be attributed to the microstructural changes including the grain growths and crack closes.

The variations of hardness and elastic modulus of specimens with heat treatment times were evaluated using indentation method according to the load–displacement or *P*–*h* curve. According to the Oliver and Pharr method[9] for a Berkovich indenter, the formulas are

$$H = P_{\max}/A, \tag{1}$$

$$E_{\mathrm{r}} = \sqrt{\pi}S/(2\beta\sqrt{A}), \tag{2}$$

in which H denotes the hardness, $P_{\max}$ is the maximum load, and A represents the contact area which is determined as $A = 24.56h_{\mathrm{c}}^2$. $h_{\mathrm{c}} = h_{\max} - \varepsilon P_{\max}/S$ is the contact depth, where $\varepsilon = 0.75$, $h_{\max}$ denotes the maximum depth, and $S = \mathrm{d}P/\mathrm{d}h$ is the contact stiffness. β is a constant depending on the indenter's geometry ($\beta = 1.034$ in the Berkovich case). E_{r} denotes the reduced Young's

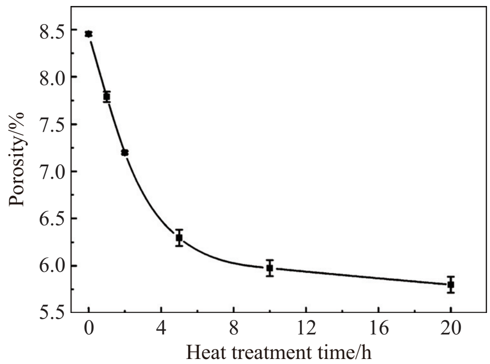

Fig. 2. The relation between porosity and heat treatment time.

modulus, which can be determined by $1/E_{\mathrm{r}} = (1-\upsilon^2)/E + (1-\upsilon_{\mathrm{i}}^2)/E_{\mathrm{i}}$, with υ and E being the Poisson's ratio and Young's modulus for the measured sample, and υ_{i} and E_{i} are Poisson's ratio and Young's modulus of the diamond indenter. Poisson's ratio is set to 0.25 for the measured sample and 0.07 for diamond indenter during this study, and E_{i} is set to 1 141 GPa. The indentation tests were carried out with the surface approach velocity being 10 nm/s, the maximum depth limit being 2 000 nm, and the holding time being 10 s, respectively.[10] The indented points can be randomly selected on the specimen surface with an optical microscopy. The size of triangle indentation was over 10 µm with 2 000 nm depth.

It is timesaving and simple to operate using the indentation technique for elastic modulus estimation of materials. However, the measured results are likely to be influenced by the microstructure since the indentation response is a combination of the indented material and structure.[11] Therefore, the Weibull distribution function (WDF) was used for data analysis to reduce errors.[12] The two-parameter WDF provides the probability f for a given parameter x as

$$f = 1 - \exp(-(x/\chi_0)^k), \quad x \geqslant 0, \tag{3}$$

where k is the Weibull modulus representing the scatter of data. The probability of i-th data can be arranged in ascending order, $f(x) = (i - 0.5)/N$. Equation (3) can be rewritten as

$$\ln(\ln(1/(1-f))) = k(\ln x - \ln \chi_0), \quad x \geqslant 0. \tag{4}$$

The parameters of k and χ_0 can be obtained by linear fitting of $\ln(\ln(1/(1-f)))$ and $\ln x$. And the characteristic value (χ_0) will be used as the final hardness (H_0) or elastic modulus (E_0) of the ceramic coating.

Figure 3 shows the Weibull distribution of some tested results on the as-received samples and those after different heat treatment times with test number $N = 20$. The hardness (H_0) and elastic modulus (E_0) can be obtained by linear fitting and calculation of the characteristic value (χ_0). The upper curve in Fig. 4 shows the relation between elastic modulus and heat treatment time. As can be seen from the graph, the elastic modulus of as-received plasma-sprayed coating is about 82.1 GPa. The value increases rapidly as the heat treatment time increases at the beginning of 5 h and increases slowly after 5 h. The elastic modulus reaches nearly 180 GPa when the heat treatment time is 20 h. In addition, the lower curve in Fig. 4 shows the relation between hardness and heat treatment time, which has a similar trend with the upper curve. The hardness increases quickly with heat treatment time in the beginning 5 h and slightly rises later. This trend agrees with the results reported in the literature.[6]

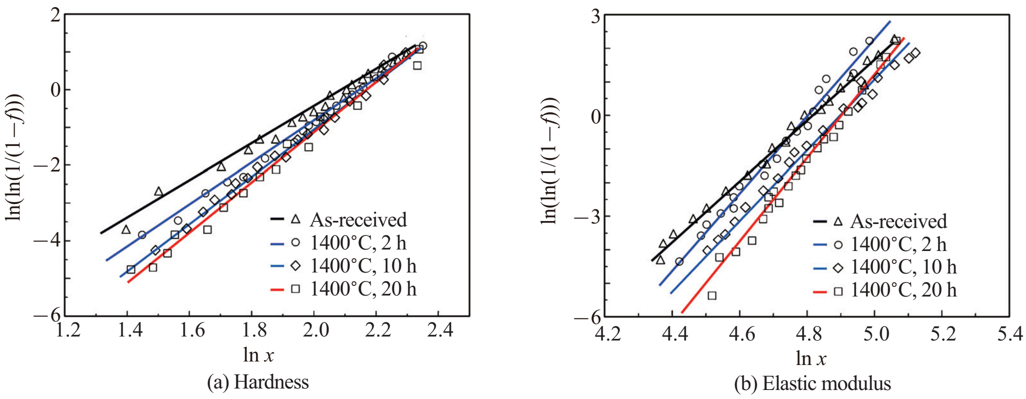

Fig. 3. Linear fitting of Weibull distribution according to the indentation test results.

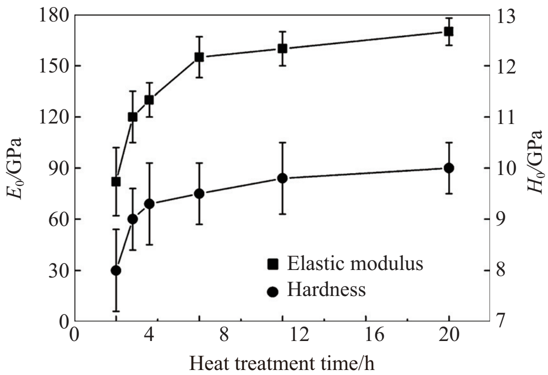

Fig. 4. Effect of heat treatment time on elastic modulus and hardness.

The mechanical properties and porosity are also studied. As shown in Fig. 5, the upper curve indicates the relation between elastic modulus and porosity, while the lower curve illustrates the relation between hardness and porosity. It can be seen from the curves that there is a sharp increase of hardness and elastic modulus when porosity decreases as for the as-received ceramic coating. The results may be caused by the sudden closure of long cracks and shape modification of pores after a short period time of high temperature treatment.[13] Furthermore, the additional part of the curves witnesses a steady increase of elastic modulus and hardness with decreasing porosity, which shows a relatively linear relation.[14] This phenomenon implies that high temperature treatment affects the elastic modulus and hardness of porous ceramic coating mainly by changing its porosity, and the effect of high temperature treatment on the elastic modulus and hardness of dense material can be ignored after a certain period of treatment time.

In conclusion, the present work presents an investigation of microstructural and mechanical

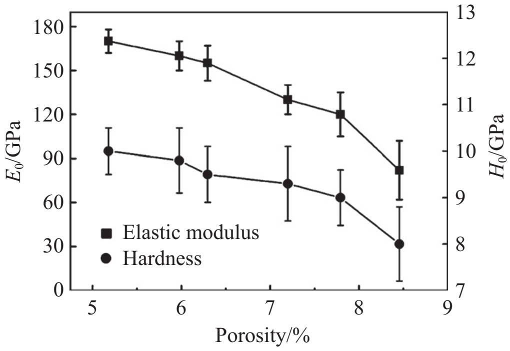

Fig. 5. Effect of porosity on elastic modulus and hardness.

properties on TBC with high temperature treatment at 1 400°C. The micro scale diagrams show that the microstructure of ceramic coating will continuously change due to the grain growths and crack closes at high temperature, and accordingly the porosity decreases with the heat treatment time. In addition, the elastic modulus and hardness increase nonlinearly with the heat treatment time and decrease with increasing porosity. This indicates that high temperature treatment affects the elastic modulus and hardness of porous ceramic coating mainly by changing its porosity, and microstructures have a significant influence on the mechanical properties of thermal barrier coating.

This work was supported by the National Natural Science Foundation of China (91216301, 11172151, 11232008, and 11372118) and the Specialized Research of Tsinghua University Initiative Scientific Research Program.

1. N. P. Padture, M. Gell, E. H. Jordan. Thermal barrier coatings for gas-turbine engine applications. *Science* **296**, 280–284 (2002).
2. C. Eberl, D. S. Gianola, X. Wang, et al. A method for in situ measurement of the elastic behavior of a columnar thermal barrier coating. *Acta Materialia* **59**, 3612–3620 (2011).
3. Y. Tan, A. Shyam, W. B. Choi, et al. Anisotropic elastic properties of thermal spray coatings determined via resonant ultrasound spectroscopy. *Acta Materialia* **58**, 5305–5315 (2010).
4. M. Alfano, G. Di Girolamo, L. Pagnotta, et al. Processing, microstructure and mechanical properties of air plasma-sprayed ceria–yttria co-stabilized zirconia coatings. *Strain* **46**, 409–418 (2010).
5. H. Y. Qi, X. G. Yang, R. Li. Interfacial fracture toughness of APS thermal barrier coating under high temperature. *Advances in Fracture and Damage Mechanics VI* **348-349**, 181–184 (2007).
6. S. Guo, Y. Kagawa. Young's moduli of zirconia top-coat and thermally grown oxide in a plasma-sprayed thermal barrier coating system. *Scripta Materialia* **50**, 1401–1406 (2004).
7. S. R. Choi, D. Zhu, R. A. Miller. Mechanical properties/database of plasma-sprayed ZrO_2-8wt% Y_2O_3 thermal barrier coatings. *International Journal of Applied Ceramic Technology* **1**, 330–342 (2004).
8. ASTM C20-00: Standard test methods for apparent porosity, water absorption, apparent specific gravity, and bulk density of burned refractory brick and shape by boiling water. ASTM, Conshohocken (2005).
9. W. C. Oliver, G. M. Pharr. An improved technique for determining hardness and elastic-modulus using load and displacement sensing indentation experiments. *Journal of Materials Research* **7**, 1564–1583 (1992).
10. J. G. Zhu, H. M. Xie, Z. X. Hu, et al. Cross-sectional residual stresses in thermal spray coatings measured by Moiré interferometry and nanoindentation technique. *Journal of Thermal Spray Technology* **21**, 810–817 (2012).
11. N. Zotov, M. Bartsch, G. Eggeler. Thermal barrier coating systems — analysis of nanoindentation curves. *Surface & Coatings Technology* **203**, 2064–2072 (2009).
12. A. Dey, A. Mukhopadhyay, S. Gangadharan, et al. Weibull modulus of nano-hardness and elastic modulus of hydroxyapatite coating. *Journal of Materials Science* **44**, 4911–4918 (2009).
13. K. Ma, J. G. Zhu, H. M. Xie, et al. Effect of porous microstructure on the elastic modulus of plasma-sprayed thermal barrier coatings: Experiment and numerical analysis. *Surface & Coatings Technology* **235**, 589–595 (2013).
14. M. Asmani, C. Kermel, A. Leriche, et al. Influence of porosity on Young's modulus and Poisson's ratio in alumina ceramics. *Journal of the European Ceramic Society* **21**, 1081–1086 (2001).